

Hydrogen bonded lambda-shaped packing motif based on 4-nitrophenylhydrazones: a promising design tool for engineering acentric crystals

Man Shing Wong,^a Volker Gramlich,^b Christian Bosshard^{*a} and Peter Günter^a

^aNonlinear Optics Laboratory, Institute of Quantum Electronics, ETH-Hönggerberg, CH-8093, Zürich, Switzerland

^bLab. für Kristallographie, ETH-Zentrum, CH-8092, Zürich, Switzerland

Two newly developed 4-nitrophenylhydrazone derivatives, 4-diethylaminobenzaldehyde 4-nitrophenylhydrazone, DEANPH, and 5-bromothiophene-2-carbaldehyde 4-nitrophenylhydrazone, BTNPH, which exhibit very strong second harmonic signals that are three orders of magnitude greater than that of the urea standard were investigated by single crystal X-ray analysis. The structural comparison with three other strongly optically nonlinear hydrazones revealed that the hydrogen bond-directed lambda-shaped supramolecular assemblies are the key and fundamental bases of all these non-centrosymmetric crystal packings. The high occurrence within this class of acentric crystals is likely due to this hydrogen bonded lambda-shaped packing motif. Since the chromophores are preferentially arranged in a lambda-shape, the acentric crystals are generally optimized for second-order nonlinear optical effects such as second harmonic generation.

The rational design and synthesis of novel crystalline materials with desirable physical properties such as electrical, optical and magnetic properties, known as crystal engineering,^{1,2} has attracted considerable attention over the last decades. The specific solid state properties often depend on the relative arrangement and orientation of the constituent functional molecules, that is the crystal structures. Unfortunately, packing arrangements of three-dimensional crystals at the molecular level are difficult to predict and control because of the interplay of various thermodynamic and kinetic contributions during the process of nucleation. In spite of such problems, important progress has recently been made in improving the predictability of crystal packing by means of limiting the degrees of freedom of the constituent molecules during the assembly of the three-dimensional crystal structures. One of the widely exploited crystal engineering approaches is to design and synthesize reliable one- or two-dimensional predefined and self-organized aggregates, supramolecular assemblies, to limit the number of possible packings and to impose a bias to the three-dimensional crystal structures. Therefore, the identification and development of useful supramolecular synthons,³ robust aggregates⁴ and packing motifs⁵ are important steps towards a successful design of functional crystalline solids.

One of the important issues to be addressed in designing useful and efficient crystalline materials for second-order nonlinear optics is how to induce a favourable acentric arrangement of the highly extended π -conjugated chromophores such as donor-acceptor disubstituted stilbenes and tolans in the solid state so that the intrinsic nonlinearities of the chromophores are maximized in the bulk. For example, in second harmonic generation (SHG), the optimal angle between the charge transfer axis of a dipolar chromophore and the polar direction of a crystal for non-critical phase matching is *ca.* 55° for the most favourable point groups.⁶ Unfortunately, in addition to the difficulty in deducing the crystal packing from the molecular structure, achiral organic molecules show an extremely high preference for a centrosymmetric packing (90%) according to a statistical survey.⁷ However, there are possible strategies that have been used to enhance the probability of forming acentric crystals which include the incorporation of molecular chirality, the introduction of structural asymmetry, the use of coulombic interaction⁸ and the use of hydrogen bonding interaction.⁹

Hydrogen bonding, owing to its relatively strong bonding strength, directionality and flexibility, is one of the most often

used non-covalent interactions to assemble supramolecular structures. A great variety of one- and two-dimensional supramolecular structures such as wires, chains, tapes, ribbons, layers and rosettes, assembled by multiple hydrogen bonds or hydrogen bond networks, have been designed and synthesized to induce a desirable crystal packing.^{4,5,10,11}

In the course of searching for useful and efficient crystalline materials based on the non-rod-shaped hydrazone skeleton, we have found that donor-substituted (hetero)aromatic aldehyde 4-nitrophenylhydrazones (Fig. 1) show an unusually high tendency to pack non-centrosymmetrically.^{12–14} Of the 28 4-nitrophenylhydrazone derivatives that have already been synthesized in our laboratory, 72% are SHG active in the Kurtz and Perry powder test which implies a non-centrosymmetric crystal packing. Furthermore, the majority of these acentric crystals (43%) exhibit very strong SHG signals that are at least two orders of magnitudes greater than that of the urea standard which implies a favourable chromophoric orientation for an efficient second harmonic generation. As a result, it would be valuable to probe and understand the packing motif of such an overwhelming bias in this class to turn this into a useful and general design tool for crystal engineering.

We report here on the molecular properties, calculated by the AM1 semi-empirical method¹⁵ and the structural properties of two newly developed hydrazones, 4-diethylaminobenzaldehyde 4-nitrophenylhydrazone, DEANPH, and 5-bromothiophene-2-carbaldehyde 4-nitrophenylhydrazone, BTNPH, which exhibit extremely strong SHG signals that are three orders of magnitude greater than that of the urea standard. In addition, the structural comparisons of these new hydrazones with three of the most optically nonlinear, acentric

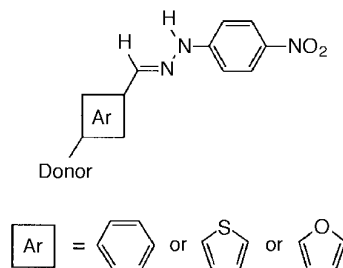


Fig. 1 Chemical structures of 4-nitrophenylhydrazone derivatives

Table 1 Molecular and structural data of 4-nitrophenylhydrazone derivatives. The molecular conformation is derived from the X-ray crystal data and the dipole moment is calculated by the AM1 semi-empirical calculation. Torsional angle refers to the twist angle between the two (hetero)aromatic rings attached on the hydrazone backbone. θ_p refers to the angles between the dipole moment of a molecule and the resultant polar direction of the corresponding crystal

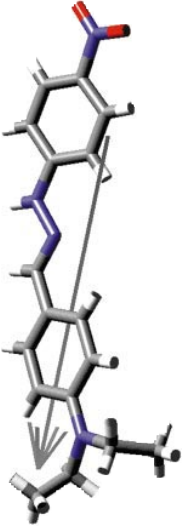
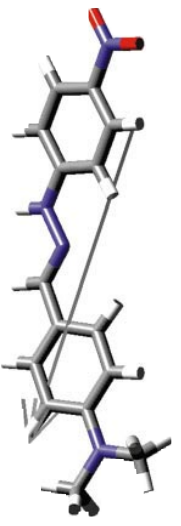

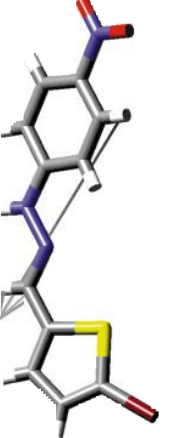
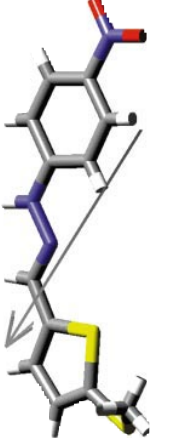
	molecular conformation and dipole orientation	dipole moment/ 10^{-29} C m	space group	point group	distance/Å of [—O...H—N—] of [—O...H—N—]	distance of [—O...H—]	torsional angle/ $^\circ$	θ_p / $^\circ$
DEANPH		3.57	<i>Pca2₁</i>	<i>mmm2</i>	3.13 (162.9)	2.25	9.1	75
DANPH		3.41	<i>Cc</i>	<i>m</i>	3.12 (147.4)	2.24	8.3	50
ACNPH		3.77	<i>Pca2₁</i>	<i>mmm2</i>	3.17 (156.4)	2.32	11.8	73
BTNPH		2.50	<i>Cc</i>	<i>m</i>	3.04 (159.8)	2.18	15.5	73
MTNPH		2.54	<i>Pca2₁</i>	<i>mmm2</i>	2.99 (162.9)	2.00	3.9	55

Table 2 Crystal data for DEANPH and BTNPH

	DEANPH	BTNPH
empirical formula	C ₁₇ H ₂₀ N ₄ O ₂	C ₁₁ H ₈ BrN ₃ O ₂ S
molecular mass	312.4	326.2
colour and habit	red fragment	red needle
crystal dimensions/mm ³	0.2 × 0.3 × 0.4	0.1 × 0.15 × 0.35
crystal system	orthorhombic	monoclinic
space group	<i>Pca</i> 2 ₁	<i>Cc</i>
point group	<i>mm</i> 2	<i>m</i>
<i>a</i> /Å	30.18(2)	4.290(2)
<i>b</i> /Å	7.320(4)	25.480(13)
<i>c</i> /Å	7.603(4)	11.832(6)
β(°)		98.12(4)
<i>v</i> /Å ³	1679.5(16)	1280.4(11)
<i>Z</i>	4	4
density/g cm ⁻³	1.235	1.692
reflections collected	1075	685
independent reflections	955	664
observed reflections	833	655
<i>F</i> (000)	664	648
parameters refined	211	170
<i>R</i> ; <i>R</i> _w (%)	5.72; 7.82	5.10; 6.63

Table 3 Bond lengths and angles for DEANPH

bond	length/Å	bonds	angle/°
N(2)–N(3)	1.378(7)	N(3)–N(2)–C(1)	112.6(5)
N(2)–C(1)	1.277(9)	C(7)–C(6)–C(5)	117.0(7)
C(6)–C(7)	1.408(12)	N(2)–N(3)–C(4)	118.5(5)
C(6)–C(5)	1.394(10)	N(3)–C(4)–C(5)	122.5(6)
N(3)–C(4)	1.389(9)	N(3)–C(4)–C(9)	116.8(6)
C(4)–C(5)	1.380(10)	C(5)–C(4)–C(9)	120.7(6)
C(4)–C(9)	1.405(9)	C(6)–C(7)–C(8)	122.3(7)
C(7)–C(8)	1.329(11)	C(6)–C(7)–N(10)	119.2(7)
C(7)–N(10)	1.466(11)	C(8)–C(7)–N(10)	118.6(7)
C(1)–C(13)	1.446(8)	N(2)–C(1)–C(13)	125.3(6)
N(19)–C(20)	1.478(11)	C(6)–C(5)–C(4)	120.3(6)
N(19)–C(16)	1.341(8)	C(20)–N(19)–C(16)	124.5(7)
N(19)–C(22)	1.532(17)	C(20)–N(19)–C(22)	116.7(6)
C(8)–C(9)	1.370(10)	C(16)–N(19)–C(22)	117.7(8)
C(20)–C(21)	1.474(13)	C(7)–C(8)–C(9)	121.7(6)
C(16)–C(17)	1.421(10)	N(19)–C(20)–C(21)	112.5(9)
C(16)–C(15)	1.398(11)	N(19)–C(16)–C(17)	122.0(7)
C(18)–C(13)	1.399(9)	N(19)–C(16)–C(15)	122.1(7)
C(18)–C(17)	1.365(9)	C(17)–C(16)–C(15)	115.9(6)
C(13)–C(14)	1.365(11)	C(13)–C(18)–C(17)	121.7(6)
O(11)–N(10)	1.242(11)	C(1)–C(13)–C(18)	123.4(6)
O(12)–N(10)	1.188(11)	C(1)–C(13)–C(14)	120.1(6)
C(14)–C(15)	1.364(10)	C(18)–C(13)–C(14)	116.5(6)
C(22)–C(23)	1.354(19)	C(16)–C(17)–C(18)	121.3(7)
C(22)–Q(1)	1.011(90)	C(4)–C(9)–C(8)	118.0(6)
C(23)–Q(1)	0.852(96)	C(13)–C(14)–C(15)	123.4(7)
		C(7)–N(10)–O(11)	115.9(8)
		C(7)–N(10)–O(12)	120.8(8)
		O(11)–N(10)–O(12)	123.2(8)
		C(16)–C(15)–C(14)	121.1(8)
		N(19)–C(22)–C(23)	112.1(15)
		N(19)–C(22)–Q(1)	142.3(55)
		C(23)–C(22)–Q(1)	38.9(54)
		C(22)–C(23)–Q(1)	48.2(59)
		C(22)–Q(1)–C(23)	92.9(78)

4-nitrophenylhydrazone crystals, DANPH,¹² ACNPH¹² and MTTNPH¹³ that were reported previously will be discussed (Table 1).

Experimental

The two new hydrazone derivatives, 4-diethylaminobenzaldehyde 4-nitrophenylhydrazone, DEANPH, and 5-bromothiophene-2-carbaldehyde 4-nitrophenylhydrazone, BTNPH, were synthesized according to the previous procedure.¹³ All the samples used for physical measurements including X-ray structure determination were grown from acetonitrile.

The melting points were determined by the differential scanning calorimetric method using a 5° min⁻¹ heating rate. The ground state molecular properties including molecular geometries and dipole moments were calculated by the AM1 semi-empirical method¹⁵ in the MOPAC6 quantum chemical calculation package.

Data collections for X-ray structure determination were performed with a Picker-Stoe diffractometer (Cu-Kα, λ = 1.54178 Å) at 293 K. The reflections were measured within 3° < 2θ < 100° with *F* > 4.0σ (*F*). The crystallographic data are summarized in Table 2. Both structures were solved by direct methods and all heavy atoms were refined by full-matrix least-squares procedures. All H atoms were located according to the riding model with fixed isotropic *U*. The bond lengths and bond angles for both DEANPH and BTNPH are in Tables 3 and 4.†

DEANPH

δ_H (300 MHz; CDCl₃; *J* values in Hz) 8.16 (d, *J* 9.27, 2H), 7.80 (s, 1H), 7.70 (s, 1H), 7.53 (d, *J* 8.94, 2H), 7.05 (d, *J* 9.21, 2H), 6.67 (d, *J* 9.00, 2H), 3.41 (q, *J* 7.08, 4H), 1.20 (t, *J* 7.08, 6H). Mp 190 °C.

BTNPH

δ_H (300 MHz, CDCl₃) 8.18 (d, *J* 9.4, 2H), 7.93 (s, 1H), 7.84 (s, 1H), 7.07 (d, *J* 9.2, 2H), 7.00 (d, *J* 3.87, 1H), 6.92 (d, *J* 3.87, 1H). Mp 189 °C.

Results and Discussion

Unlike the stilbene derivatives, all the 4-nitrophenylhydrazone derivatives adopt a non-rod-shaped conformation in the crystalline state due to the bent hydrazone backbone (–CH=N\NH–) as examined from the molecular structures (see Table 1). The electron-withdrawing group, the 4-nitrophenyl ring and the electron-donating group, the donor-substituted

† Atomic coordinates, thermal parameters, and bond lengths and angles have been deposited at the Cambridge Crystallographic Data Centre (CCDC). See Information for Authors, *J. Mater. Chem.*, 1997, Issue 1. Any request to the CCDC for this material should quote the full literature citation and the reference number 1145/44.

Table 4 Bond lengths and angles for BTNPH

bond	length/Å	bonds	angle/°
Br–C(4)	1.911(12)	C(1)–S–C(4)	89.5(5)
S–C(1)	1.734(9)	C(12)–C(13)–C(8)	120.3(9)
S–C(4)	1.714(12)	C(1)–C(2)–C(3)	111.5(10)
C(13)–C(12)	1.367(13)	C(12)–C(11)–N	119.4(9)
C(13)–C(8)	1.417(13)	C(12)–C(11)–C(10)	122.2(8)
C(2)–C(1)	1.365(15)	N–C(11)–C(10)	118.4(8)
C(2)–C(3)	1.379(18)	C(1)–C(5)–N(6)	119.9(9)
C(11)–C(12)	1.375(13)	S–C(1)–C(2)	112.0(8)
C(11)–N	1.488(12)	S–C(1)–C(5)	121.1(7)
C(11)–C(10)	1.375(14)	C(2)–C(1)–C(5)	126.9(9)
C(5)–C(1)	1.417(14)	C(13)–C(12)–C(11)	118.7(9)
C(5)–N(6)	1.318(13)	C(13)–C(8)–C(9)	118.2(8)
C(8)–C(9)	1.391(12)	C(13)–C(8)–N(7)	117.6(8)
C(8)–N(7)	1.342(12)	C(9)–C(8)–N(7)	124.1(9)
C(9)–C(10)	1.349(13)	C(8)–C(9)–C(10)	121.4(9)
C(4)–C(3)	1.326(18)	Br–C(4)–S	117.6(7)
N–O(2)	1.210(12)	Br–C(4)–C(3)	129.7(10)
N–O(2)	1.219(14)	S–C(4)–C(3)	112.7(9)
N(6)–N(7)	1.364(12)	C(2)–C(3)–C(4)	114.4(12)
		O(2)–N–C(11)	119.4(9)
		O(2)–N–O(2)	123.2(9)
		C(11)–N–O(2)	117.4(9)
		C(5)–N(6)–N(7)	119.5(8)
		C(11)–C(10)–C(9)	119.2(8)
		C(8)–N(7)–N(6)	119.5(8)

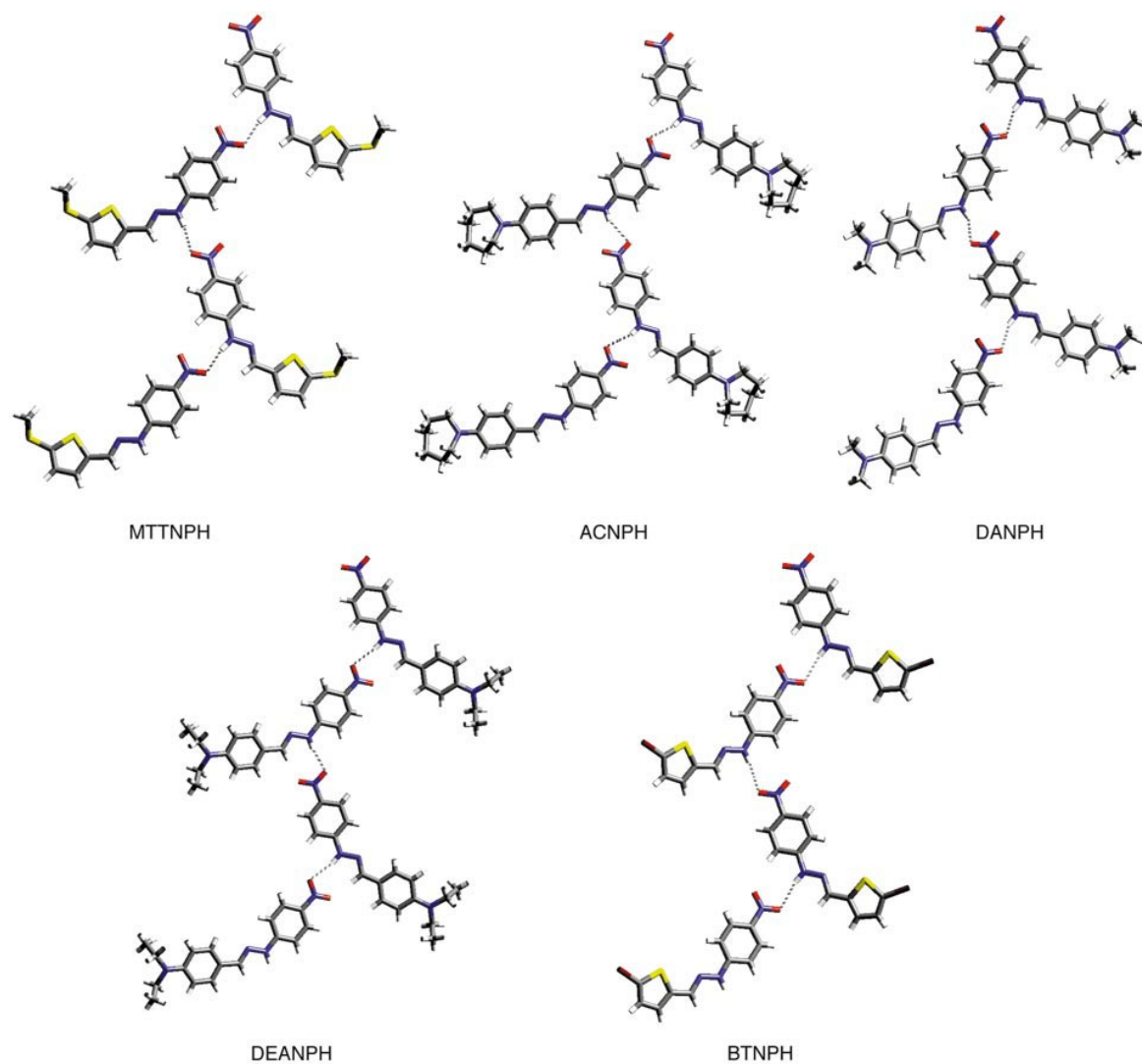


Fig. 2 The hydrogen bonded lambda-shaped molecular assemblies found in the crystalline solids of DEANPH, DANPH, ACNPH, BTNPH and MTTNPH. The dotted line represents the hydrogen bond. For clarity, the view is not along a crystal axis.

hetero(aromatic) ring that are attached to the hydrazone backbone generally show a good co-planarity. This is an essential conformation for an efficient delocalization of π -electrons along the entire hydrazone skeleton and thus ensures the desirable solid-state properties such as large macroscopic nonlinear optical properties. The optimized molecular geometries of all these hydrazone derivatives, calculated by the AM1 semi-empirical method, are in a good agreement with those found in the crystalline state with an exception of the conformation of the $-\text{NH}-$ part. The conformation of $-\text{NH}-$ in the optimized geometry is pyramidal. On the other hand, the solid-state structures show an excellent planarity of the hydrazone bridge. The calculated dipole moments are very large for all these 4-nitrophenylhydrazone derivatives. The dipole orientations are strongly dependent on the molecular conformation and not always directed along the molecular plane as shown in Table 1.

As revealed from the single crystal X-ray structures, the packing modes of all the investigated 4-nitrophenylhydrazone derivatives are very similar and only fall into two non-centrosymmetric space groups: $Pca2_1$ and Cc . Impressively, the one-dimensional, lambda-shaped molecular assemblies, which are composed of the glide plane-related molecules and held together by the hydrogen bonds between the nitro oxygen

and the amino proton, were found to be the key and common characteristics of all these acentric crystal structures (Fig. 2). Although the $\text{O}\cdots\text{N}$ distances ($>3.0 \text{ \AA}$) and the $\text{O}\cdots\text{H}$ bond lengths ($>2.0 \text{ \AA}$) are relatively long, implying relatively weak hydrogen bonds, the co-operative effect of the hydrogen bond network is believed to play an important role in stabilizing the assembly. In addition, these lambda-shaped molecular assemblies stack up with a different extent of offset from the adjacent assemblies at a van der Waals distance ($>3.5 \text{ \AA}$) forming two-dimensional acentric layers as shown in Fig. 3. Finally, for those molecules packing in space group $Pca2_1$, i.e. DEANPH, ACNPH and MTTNPH, the two-dimensional acentric layers arrange in an anti-parallel fashion giving rise to the three-dimensional crystal structure shown in Fig. 4. Since the molecules do not lie parallel to the planes of a unit cell, this leads to a net dipole along the crystallographic c axis as a resultant polar axis. In contrast, the two-dimensional acentric layers of BTNPH and DANPH (space group Cc) pack in a parallel manner resulting in the crystal structures as shown in Fig. 5. Similar to the previous case, as the molecules do not lie parallel to the planes of a unit cell, the crystallographic a -axis and c -axis are polar axes of these packings, respectively.

The angles, θ_p , between the dipole moment of a molecule and the resultant polar direction of the hydrazone crystals are

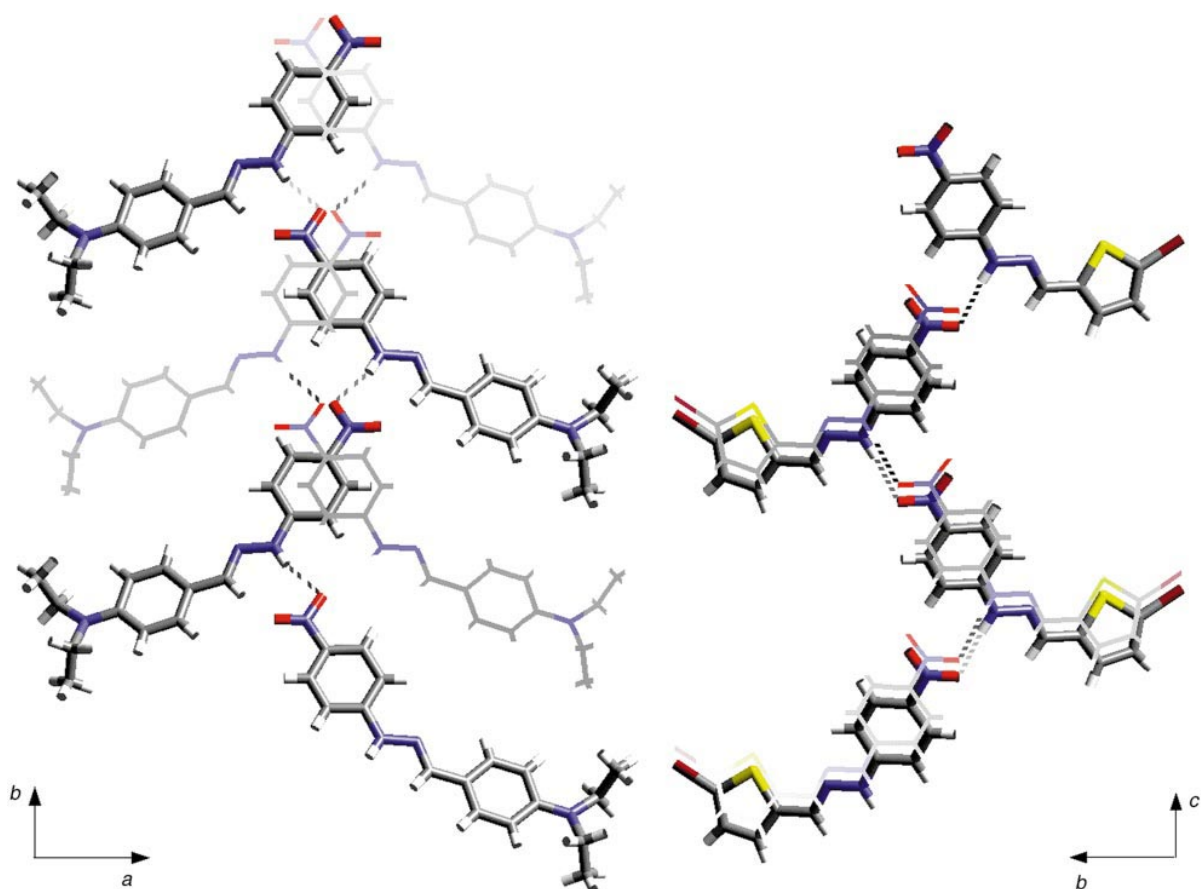


Fig. 3 The relative arrangement of the two lambda-shaped molecular assemblies of DEANPH and BTNPH in the crystalline states. The dotted line represents the hydrogen bond. For clarity, the layers in the foreground are represented by the stick model and the layers in the background are represented by the cylindrical model.

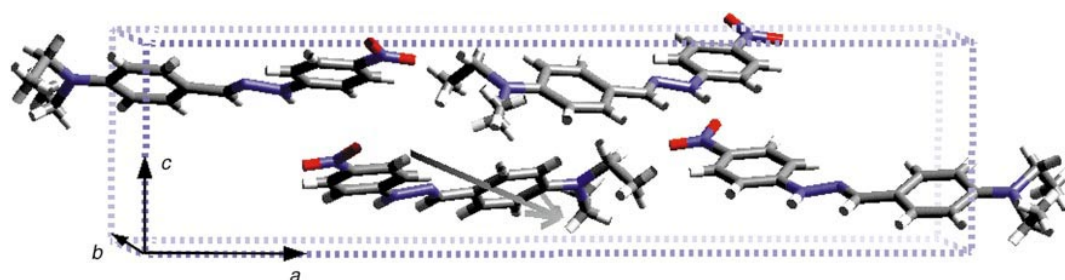


Fig. 4 Crystal packing of DEANPH in a unit cell. The arrow represents the permanent dipole calculated by the AM 1 semi-empirical calculations.

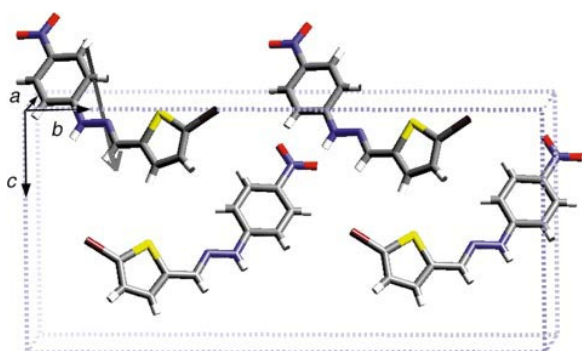


Fig. 5 Crystal packing of BTNPH in a unit cell. The arrow represents the permanent dipole calculated by the AM 1 semi-empirical calculations.

listed in Table 1. Interestingly, all these hydrazone derivatives show very favourable chromophoric arrangements for large nonlinear optical effects such as SHG, especially MTNPH, which even has the optimal chromophoric orientation for highly efficient nonlinear optical effects. In addition to the large molecular hyperpolarizabilities,^{12,13} such a highly favourable chromophoric arrangement can explain the very strong activities of these hydrazone crystals in the powder test.

Conclusions

In summary, the donor-substituted (hetero)aromatic aldehyde 4-nitrophenyl-hydrazone derivatives show an overwhelmingly high propensity for a non-centrosymmetric packing in spite of their large permanent dipoles. In view of the five strongly SHG active single crystal X-ray structures, the hydrogen bonded lambda-shaped molecular assemblies provide a common and fundamental basis for all these non-centrosymmetric structures.

Because of the preferential lambda-shaped arrangement of the chromophores, the crystals formed are especially suitable and optimized for nonlinear optical effects. As a result, the hydrogen bonded lambda-shaped packing motif is a very useful design tool for engineering acentric crystals.

This work was supported in part by the Swiss National Science Foundation. We thank Rolf Spreiter for the determination of the angles θ_p .

References

- 1 G. R. Desiraju, *Crystal Engineering*, Elsevier, Amsterdam, 1989.
- 2 G. M. J. Schmidt, *Pure Appl. Chem.*, 1971, **27**, 647.
- 3 G. R. Desiraju, *Angew. Chem., Int. Ed. Engl.*, 1995, 2311.
- 4 V. A. Russell and M. D. Ward, *Chem. Mater.*, 1996, **8**, 1654.
- 5 J. C. MacDonald and G. M. Whitesides, *Chem. Rev.*, 1994, 2383.
- 6 J. F. Nicoud and R. J. Twieg, in *Nonlinear Optical Properties of Organic Molecules and Crystals*, ed. D. S. Chemla and J. Zyss, Academic Press, Orlando, 1987, p. 227.
- 7 J. Jacques, A. Collet and S. H. Wilen, *Enantiomers Racemates and Resolutions*, Wiley, New York, 1981.
- 8 S. R. Marder and J. W. Perry, *Adv. Mater.*, 1993, **5**, 804.
- 9 M. C. Etter, G. M. Frankenbach and D. A. Adsmund, *Mol. Cryst. Liq. Cryst.*, 1990, **187**, 22.
- 10 C. B. Aakeröy and K. R. Seddon, *Chem. Soc. Rev.*, 1993, 397.
- 11 M. S. Wong, F. Pan, V. Gramlich, C. Bosshard and P. Günter, *Adv. Mater.*, 1997, **9**, 554.
- 12 C. Serbutoviez, C. Bosshard, G. Knöpfle, P. Wyss, P. Prêtre, P. Günter, K. Schenk, E. Solari and G. Chapuis, *Chem. Mater.*, 1995, **7**, 1198.
- 13 M. S. Wong, U. Meier, F. Pan, C. Bosshard, V. Gramlich and P. Günter, *Adv. Mater.*, 1996, **8**, 416.
- 14 M. S. Wong, C. Bosshard, F. Pan and P. Günter, *Adv. Mater.*, 1996, **8**, 677.
- 15 M. J. S. Dewar, E. G. Zoebisch, E. F. Healy and J. P. Stewart, *J. Am. Chem. Soc.*, 1985, **107**, 3902.

Paper 7/02339A; Received 7th April, 1997